

Prospective Evaluation of an Amide-Based Zinc Scaffold as an Anti-Alzheimer Agent: *In Vitro*, *In Vivo*, and Computational Studies

Wajeeha Waseem, Fareeha Anwar,* Uzma Saleem, Bashir Ahmad, Rehman Zafar, Asifa Anwar, Muhammad Saeed Jan, Umer Rashid, Abdul Sadiq, and Tariq Ismail



Cite This: *ACS Omega* 2022, 7, 26723–26737



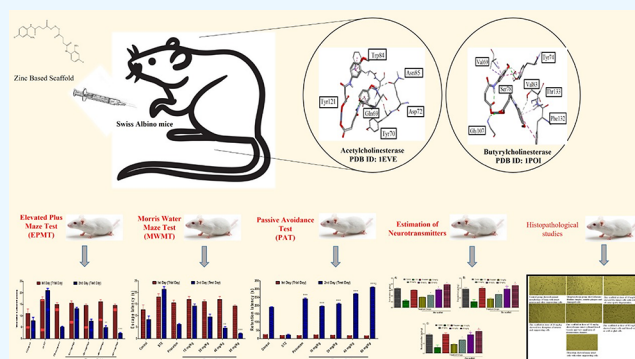
Read Online

ACCESS |

Metrics & More

Article Recommendations

ABSTRACT: Alzheimer's disease is the most common progressive neurodegenerative mental disorder associated with loss of memory, decline in cognitive function, and dysfunction of language. The prominent pathogenic causes of this disease involve deposition of amyloid- β plaques, acetylcholine neurotransmitter deficiency, and accumulation of neurofibrillary tangles. There are multiple pathways that have been targeted to treat this disease. The inhibition of the intracellular cyclic AMP regulator phosphodiesterase IV causes the increase in cAMP levels that play an important role in the memory formation process. Organometallic chemistry works in a different way in treating pharmacological disorders. In the field of medicinal chemistry and pharmaceuticals, zinc-based amide carboxylates have been shown to be a preferred pharmacophore. The purpose of this research work was to investigate the potential of zinc amide carboxylates in inhibition of phosphodiesterase IV for the Alzheimer's disease management. Swiss Albino mice under controlled conditions were divided into seven groups with 10 mice each. Group I was injected with carboxymethylcellulose (CMC) at 1 mL/100 g dose, group II was injected with Streptozotocin (STZ) at 3 mg/kg dose, group III was injected with Piracetam acting as a standard drug at 200 mg/kg dosage, while groups IV–VII were injected with a zinc scaffold at the dose regimen of 10, 20, 40, and 80 mg/kg through intraperitoneal injection. All groups except group I were injected with Streptozotocin on the first day and third day of treatment at the dose of 3 mg/kg through an intracerebroventricular route to induce Alzheimer's disease. Afterward, respective treatment was continued for all groups for 23 days. In between the treatment regimen, groups were analyzed for memory and learning improvement through various behavioral tests such as open field, elevated plus maze, Morris water maze, and passive avoidance tests. At the end of the study, different biochemical markers in the brain were estimated like neurotransmitters (dopamine, serotonin and adrenaline), oxidative stress markers (superoxide dismutase, glutathione, and catalase), acetylcholinesterase (AChE), tau proteins, and amyloid- β levels. A PCR study was also performed. Results showed that the LD₅₀ of the zinc scaffold is greater than 2000 mg/kg. Research indicated that the zinc scaffold has the potential to improve the memory impairment and learning behavior in Alzheimer's disease animal models in a dose-dependent manner. At the dose of 80 mg/kg, a maximum response was observed for the zinc scaffold. Maximum reduction in the acetylcholinesterase enzyme was observed at 80 mg/kg dose, which was further strengthened and verified by the PCR study. Oxidative stress was restored by the zinc scaffold due to the significant activation of the endogenous antioxidant enzymes. This research ended up with the conclusion that the zinc-based amide carboxylate scaffold has the potential to improve behavioral disturbances and vary the biochemical markers in the brain.



INTRODUCTION

Alzheimer's disease is the most prevalent kind of dementia, accounting for 55 to 60% of all cases.¹ Alzheimer's disease is a growing neurodegenerative disorder of the brain that causes memory loss and is accompanied by signs and symptoms as well as behavioral changes.² Memory loss is the first symptom of this illness. Dementia, often known as forgetfulness, is the generic term for the loss of cognitive and memory abilities that significantly disrupts everyday activities. Mixed dementia, lev

bodies, vascular dementia, Alzheimer's disease, frontal temporal dementia, and Parkinson's disease are all frequent kinds of

Received: May 16, 2022

Accepted: July 4, 2022

Published: July 19, 2022



Table 1. Cholinesterase Inhibitory Potential of the Zinc-Based Scaffold and Standard Drug^a

compound	concentration ($\mu\text{g/mL}$)	% AChE activity	IC ₅₀ ($\mu\text{g/mL}$)	% BChE activity	IC ₅₀ ($\mu\text{g/mL}$)
zinc-based scaffold	1000	88.58 \pm 1.12**	26.5	78.76 \pm 0.71*	44.60
	500	81.65 \pm 1.34*		71.23 \pm 1.83*	
	250	74.31 \pm 2.15 ^{ns}		66.42 \pm 0.43**	
	125	67.56 \pm 1.73***		60.56 \pm 1.06**	
	62.5	62.44 \pm 0.58*		55.80 \pm 1.50***	
Galantamine	1000	94.40 \pm 0.03	7.80	82.33 \pm 1.20	4.06
	500	85.03 \pm 2.16		76.33 \pm 0.95	
	250	80.90 \pm 1.11		72.67 \pm 0.91	
	125	76.44 \pm 0.28		70.00 \pm 0.17	
	62.5	71.22 \pm 0.47		68.60 \pm 0.04	

^aRepresentation of data as mean \pm standard error of the mean; significant differences from the positive control as follows: superscript ns, nonsignificant; * $P < 0.05$, ** $P < 0.01$, and *** $P < 0.001$; $n = 3$.

dementia.³ The usage of acetylcholinesterase inhibitors is widespread. Acetylcholinesterase reduction is the depletion in enzyme activity in Alzheimer's disease that prevents the breakdown of acetylcholine (ACh), which is present in the AD brain.⁴ Many hypotheses have been proposed in relation to pathogenic variables in Alzheimer's disease. Reduced cholinergic activity, detection of proteins such as amyloid- β ($A\beta$), and neurofibrillary tangles (also termed as tau proteins) in neuronal areas of the nervous system are examples. Consequently, medications, largely by inhibiting β -secretase (BACE-1), boost the intensity of acetylcholine (ACh), reducing the development of harmful $A\beta$ peptides, and are being considered for the development of anti-AD therapies. Since an anticholinergic is indeed a simple and effective indicator of incursion from the perception of pharmacology, it may be utilized.⁵

Neurofibrillary tangles (NFTs) are hyperphosphorylated tau proteins that are found in many areas of the brain and are native in filament form. Inside nerves, the proteins (tau) perform a crucial function as mitotic spindle-stabilizing mediators in normal circumstances. However, in Alzheimer's patients, abnormal hyperphosphorylation of tau proteins occurs, resulting in microtubule breaking and subsequent expansion in brain regions.⁶ Natural ingredients have been used to treat Alzheimer's disease in various scientific trials. Tau base proteins, according to recent research, are an effective drug for offering relief to patients with Alzheimer's disease, and they have also been recommended as a therapeutic approach for the condition. Different natural therapies produced from creatures including algae, plants, and invertebrates have been shown to be active in tau-related tests.⁷ Researchers were interested in ethnobotanical plants for the treatment of neurological diseases. Many plants have developed active proteins with the potential to be used in the creation of medication.⁸ According to overwhelming evidence, brain tissues in Alzheimer's disease patients are subjected to peroxidation during the illness's progression. Protein oxidation, lipid oxidation, DNA oxidative stress, and glycooxidation, among other forms of osmotic damage or harm, are all implicated in the prognosis of Alzheimer's disease.⁹ Nerve cell death, synaptic injury, the creation and buildup of $A\beta$ plaques formed from intracellular NFTs and APP processing made of accumulated hyperphosphorylated tau proteins inside the brain, astrocyte multiplication, and microglial activation are all symptoms of Alzheimer's disease.¹⁰ Due to their therapeutic character, synthetic chemicals, together with medicinal plants, have played an important part in the treatment of many ailments throughout history. Despite the fact that an allopathic system of medicine provides a radial therapy for Alzheimer's disease, the

universe is moving toward investigating the use of synthetic medications for Alzheimer's disease treatment. Pharmacological actions related to various functional groups and substituents such as anticancer, antiseptic, analgesic, antiviral, and anticholinergic actions have been observed in numerous manufactured pharmaceutical compounds.¹¹ None of the present Alzheimer's derangement curative therapies (medications) postpone or prevent the weakening and loss of neurons that produce Alzheimer's indicators and lead to death.¹² Donepezil, Galantamine, Memantine, Rivastigmine, Memantine paired with Donepezil, and Tacrine have all been authorized by the US Food and Drug Administration (FDA) for the management of Alzheimer ailment. (Tacrine has been withdrawn in the United States.) Organometallic chemistry involves the class of compounds that contain at least one or two interacting bonds between the carbon atom and the metallic element like silicon, iron, cobalt, nickel, zinc, boron, etc.¹³ These types of compounds have the capacity to perform a number of pharmacological and nonpharmacological functions. These types of compounds have been utilized since the beginning to treat multiple illnesses like viral, bacterial, leishmanial, and other contagious infections.¹⁴ This field had been a magical discovery after the synthesis of cisplatin, the anticancerous drug that proved the antitumor behavior of these types of compounds. Zinc, copper, and iron have been found with improved pharmacological importance in our body, and lack of any one of these can lead to decreased immunity and development of bizarre and diminished ability of a person toward a normal body working.¹⁵ A number of zinc-based scaffolds have been reported to be used in medicinal chemistry for a longer period of time as therapeutic moieties.¹⁶ These metal scaffold derivatives were applied for treatment of cancerous diseases to recover from inflammation, for the management of diabetes mellitus and microbial diseases, and in the therapy of specific conditions, such as Huntington's disease, heart diseases, and genetic diseases, among others. The use of metal complexes as an effective therapeutic entity shows that it is possible to minimize toxicity at the cellular level by selecting a suitable ligand.¹⁷

Zinc has been involved in a number of biological functions in the human body like preservation of metabolism, DNA functioning, signal transduction, and cell growth.¹⁸ As the size and charge on the zinc metal are compatible with proteins in the human body, it is utilized by a variety of proteins to stabilize the structure.¹⁹ The proteins that consume zinc are mostly transcription factors and enzymes that have high molecular weight. Zinc is responsible for speeding up enzymatic reaction in immunological processes such as the wound healing process and

Table 2. Free Radical Scavenging Potential Activities of the Zinc-Based Scaffold^a

sample	con. ($\mu\text{g/mL}$)	% DPPH activity	IC ₅₀ ($\mu\text{g/mL}$)	% ABTS activity	IC ₅₀ ($\mu\text{g/mL}$)	% H ₂ O ₂ activity	IC ₅₀ ($\mu\text{g/mL}$)
zinc-based scaffold	1000	93.10 \pm 0.60 ^{ns}	5.34	82.33 \pm 1.20 ^{***}	4.06	78.08 \pm 1.04 ^{***}	35.10
	500	87.58 \pm 0.63 ^{ns}		76.33 \pm 0.95 ^{***}		71.45 \pm 0.90 ^{***}	
	250	83.76 \pm 0.71 ^{ns}					
	125	75.44 \pm 0.58 ^{ns}		72.67 \pm 0.91 ^{***}		66.58 \pm 0.63 ^{***}	
	62.5	68.10 \pm 0.90 ^{ns}		70.00 \pm 0.17 ^{***}		61.40 \pm 0.20 ^{***}	
				68.60 \pm 0.04 ^{***}		56.80 \pm 0.90 ^{***}	
ascorbic acid	1000	94.40 \pm 0.03	5.80	91.90 \pm 0.96	3.23	95.23 \pm 0.22	13.72
	500	85.03 \pm 2.16		87.08 \pm 0.47		89.45 \pm 0.90	
	250	80.90 \pm 1.11		82.40 \pm 0.20		83.90 \pm 0.60	
	125	76.44 \pm 0.28		77.61 \pm 0.43		77.00 \pm 0.30	
	62.5	71.22 \pm 0.47		75.45 \pm 0.90		72.90 \pm 0.45	

^aRepresentation of data as mean \pm standard error of the mean; significant differences from the positive control as follows: superscript ns, nonsignificant; * $P < 0.05$, ** $P < 0.01$, and *** $P < 0.001$; $n = 3$.

DNA functioning. In pregnant women, zinc is also needed for the normal growth of fetus. Thus, lack of this important mineral can result in genetic alteration, delayed sexual maturity, delayed or impaired wound healing, chronic diarrhea, skin rashes, behavioral issues, etc.²⁰ On the basis of the scientific evidence on the role of zinc in biological activities, this study was designed to find out the anti-Alzheimer potential of the newly synthesized zinc scaffold as zinc is necessary for many body functions including cognitive abilities.

RESULTS

In Vitro Assays. Cholinesterase Assays. Table 1 shows the results of acetylcholinesterase and butyl cholinesterase inhibition by various doses of the zinc-based scaffold, and Galantamine dose-dependently inhibited the AChE enzyme with the IC₅₀ value range of 26.5 to 7.80 $\mu\text{g/mL}$ correspondingly. Likewise, the zinc-based scaffold causes BChE enzyme inhibition, giving IC₅₀ values of 44.60 and 4.06 $\mu\text{g/mL}$ (Table 1).

Formulas for AChE and BChE inhibition by a compound involve $V = \Delta \text{Abs} / \Delta t$, % enzyme activity = $V / V_{\text{max}} \times 100$, and % enzyme inhibition = $100 - \% \text{ enzyme activity}$ (V (sample) represents the reaction rate with an inhibitor, and V_{max} (control) represents the reaction rate without inhibition). Values of control include the absorbance on a UV–Visible spectrophotometer as $A-1 = 0.734$ and $A-2 = 0.884$.

ABTS Free Radical Scavenging Activity. In this type of assay, the zinc-based scaffold displayed % ABTS inhibition values of 82.33 ± 1.20 , 76.33 ± 0.95 , 72.67 ± 0.91 , 70.00 ± 0.17 , and 68.60 ± 0.04 with an IC₅₀ value of 4.06 $\mu\text{g/mL}$ at concentrations of 1000, 500, 250, 125, and 62.5 $\mu\text{g/mL}$, respectively. The % ABTS inhibition of the zinc-based scaffold was compared with that of the positive control, which was ascorbic acid and revealed a concentration-dependent reaction. Ascorbic acid showed 91.90 \pm 0.96 inhibition at a concentration of 1000 $\mu\text{g/mL}$ against ABTS with an IC₅₀ value of 3.23 $\mu\text{g/mL}$ as tabulated in Table 2. The formula for the scavenging free radical by a compound is % radical scavenging, = $A - B/A \times 100$, where A is the control absorbance and B is the sample absorbance.

DPPH Free Radical Scavenging Potential. The DPPH free radical scavenging, potential values of the zinc-based scaffold were 93.10 ± 0.60 , 87.58 ± 0.63 , 83.76 ± 0.71 , 75.44 ± 0.58 , and 68.10 ± 0.90 with the IC₅₀ value of about 5.34 $\mu\text{g/mL}$ in the concentrations of about 1000, 500, 250, 125, and 62.5 $\mu\text{g/mL}$, respectively (Table 2). Ascorbic acid indicated 94.40 ± 0.03 inhibition at the concentration of about 1000 $\mu\text{g/mL}$ against

DPPH with the IC₅₀ value of 5.80 $\mu\text{g/mL}$. The formula for the scavenging free radical by a compound is % radical scavenging, = $A - B/A \times 100$, where A is the control absorbance and B is the sample absorbance (the control value is $A = 0.723$).

Hydrogen Peroxide Free Radical Scavenging Potential. The H₂O₂ free radical scavenging, potential values of the zinc-based scaffold were 78.08 ± 1.04 , 71.45 ± 0.90 , 66.58 ± 0.63 , 61.40 ± 0.20 , and 56.80 ± 0.90 with the IC₅₀ value of about 35.10 $\mu\text{g/mL}$ in the concentrations of about 1000, 500, 250, 125, and 62.5 $\mu\text{g/mL}$, respectively. Ascorbic acid indicated 95.23 ± 0.22 inhibition at the concentration of about 1000 $\mu\text{g/mL}$ against H₂O₂ with the IC₅₀ value of 13.72 $\mu\text{g/mL}$ (Table 2).

The formula for the scavenging free radical by a compound is % radical scavenging = $A - B/A \times 100$, where A is the control absorbance and B is the sample absorbance (the control value is $A = 0.723$).

Zinc-Based Scaffold Effects on Acute Toxicity. The zinc-based scaffold was observed at the doses of about 50, 100, 200, 300, and up to 2000 mg/kg. Behavioral properties of the zinc-based scaffold were notable for the individual mice at about 0, 30, 60, and 120 min, 24, 48, and 72 h, and 1 week after the I/P administration of the drug as given in Table 3. During a study, no

Table 3. Analysis of Acute Toxicity of Animals after Administration of the Synthesized Zinc Scaffold

group	animals	zinc scaffold (mg/kg)
1	8	5
2	8	25
3	8	50
4	8	100
5	8	200
6	8	300
7	8	400
8	8	500
9	8	1000
10	8	2000

acute toxicity was detected at any stage, as measured by distinct mortality, respiratory discomfort (cyanosis or gasping), changed reflex behaviors, and the absence of convulsions. After 30 and 60 min of administration/injection, the fleeing behavior and spontaneous activity in four of the six animals/mice were stronger than previously at dosages of around 10 and 50 mg/kg. There was most likely an enhancement in allergic reaction (measured as aggressive behavior during treatment and a

Table 4. Results of Open Field Testing by the Zinc-Based Scaffold and Standard Controls^a

treatment group	latency time (s)	rearing (no.)	freezing time (s)	no. of crossings	time spent in the periphery (s)	time spent in the center (s)	defecation
zinc scaffold (10 mg/kg)	4.6 ± 0.6	4.4 ± 0.4	134 ± 1.5*	18.2 ± 1.4	158 ± 0.9	3.1 ± 0.7	no
zinc scaffold (20 mg/kg)	3.7 ± 0.2*	10.2 ± 0.6	102 ± 0.9*	31.0 ± 1.6	147 ± 0.6	5.4 ± 0.4*	yes
zinc scaffold (40 mg/kg)	2.1 ± 0.1*	14.6 ± 0.2*	80 ± 1.4*	38.2 ± 1.1*	107 ± 0.5*	7.7 ± 0.7*	no
zinc scaffold (80 mg/kg)	1.0 ± 0.0* ^{#,α}	16.2 ± 1.4* ^{#,α}	52 ± 1.8* ^{#,α}	47.1 ± 1.1* ^α	98 ± 1.2* [#]	9.1 ± 0.9* ^{#,α}	yes
control	2.9 ± 0.3	9.2 ± 0.8	72 ± 1.4	39.7 ± 0.7	123.2 ± 1.3	7.3 ± 0.4	yes
Streptozotocin	6.2 ± 0.6 [#]	2.6 ± 0.2 [#]	156 ± 1.7 [#]	16.2 ± 1.2 [#]	161.2 ± 1.1 [#]	2.7 ± 0.1 [#]	yes
Piracetam	2.2 ± 0.4*	6.2 ± 0.4	82 ± 0.7*	29.3 ± 1.1	122.6 ± 1.6	6.4 ± 0.5*	yes

^aRepresentation of data as mean ± standard error of the mean; significant differences from the disease control: ns, nonsignificant; **P* < 0.05; *n* = 10; [#]*P* < 0.05 vs control; ^α*P* < 0.05 vs piracetam.

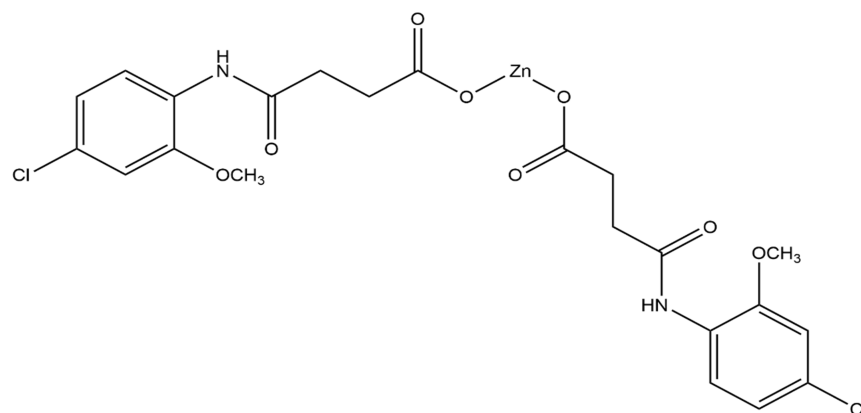


Figure 1. Structure of the synthesized zinc scaffold.

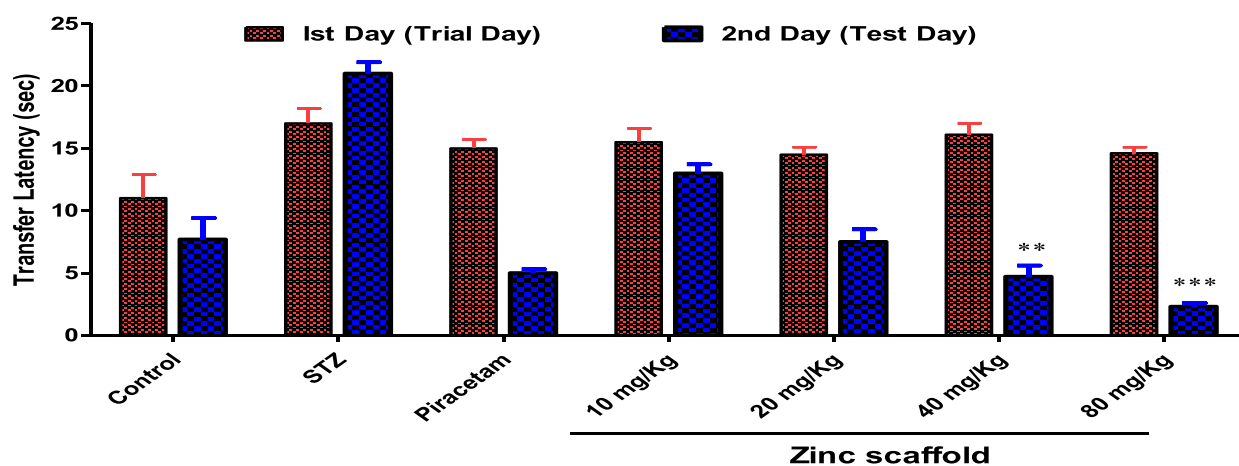


Figure 2. Effect of the zinc-based scaffold at variable doses on transfer latency (s) in the elevated plus maze test. Representation of data as mean ± standard error of the mean; significant differences from the disease control as follows: ***P* < 0.01 and ****P* < 0.001; *n* = 10.

substantial rise in irritation), and the escape performance in the same animals/mice was also higher. At a dosage greater than 500 mg per kg, five of the six animals/mice were found to be drowsy. At 24 h to 1 week following the administration/injection, all of the animals/mice seemed normal, with no noticeable changes in their behavior, activity, or appearance.

Behavioral Studies on Animals. Open Field Test (OFT). When the synthesized zinc-based chemical moiety was analyzed for open field test, this compound gave satisfactory outputs at the given dose of 80 mg/kg with a prominent decline in the latency time of animals in comparison with the control

(positive) group and Streptozotocin-treated group. Afterward, when this compound was analyzed further, it displayed the dose-dependent upsurge in locomotor activities, for example, increasing the dose results in an increase in freezing time, with a decrease in the number of crossings. Animals prefer to spare more time in the central radius compared with the time spent on the periphery. This enhancement of time was due to the effect of the chemical moiety on the testing animals. Results are elaborated in Table 4.

Elevated Plus Maze Test (EPMT). The transfer latency (TL) on the second day demonstrated that the learnt task or memory

had been retained. Compared to the positive control group, all of the young animals/mice treated with the zinc-based scaffold at dosages of 10, 20, 40, and 80 mg/kg (I/P) showed a dose-dependent drop in the TL on the second day, indicating a substantial improvement in memory. These concentrations of the zinc-based scaffold (10, 20, 40, and 80 mg/kg, I/P) also created a major progress in the cognition or memory ($P < 0.001$) of the older mice (Figure 2). Before training, a positive control was given, and it significantly increased ($P < 0.01$) the transfer latency (TL) on the second day, showing impairment in cognition or memory, as evaluated by the time it took for the mouse or animal to shut its arms with all four legs. On the first day, TL made a note of each animal's training session. The animal/mouse was given another 2 min to explore the raised plus labyrinth before being returned to its home cage. The mouse's ability to retain this learnt job (memory) was assessed for 24 h after the first day, which is known as the trial day. Improvement in cognition or memory was indicated by a significant decrease in the TL value range of the retention. Results are tabulated in Table 5.

Table 5. Elevated Plus Maze Test Values with Entries in Open and Closed Arms^a

drug treatment groups	open arm time spent	closed arm time spent
control group	9.2 ± 1.3	153 ± 1.1
Streptozotocin group	5.1 ± 1.5 [#]	192 ± 1.6 [#]
Piracetam (200 mg/kg)	8.8 ± 0.7*	156 ± 1.4*
zinc scaffold (10 mg/kg)	6.3 ± 1.1*	173 ± 0.3*
zinc scaffold (20 mg/kg)	7.5 ± 0.2*	165 ± 1.5*
zinc scaffold (40 mg/kg)	8.2 ± 1.4*	143 ± 1.4*
zinc scaffold (80 mg/kg)	9.5 ± 0.9*	133 ± 0.9*

^aRepresentation of data as mean ± standard error of the mean; significant difference from the disease control as follows: * $P < 0.05$; $n = 10$; [#] $P < 0.05$ vs control.

Effect of the Zinc-Based Scaffold in the Morris Water Maze Test (MWM). Morris water maze test was proved extremely useful in revealing problems with dimensional remembrance and learning. The enactment of all groups of mice increased throughout the experimental phase, as seen by the reduction in escape latency over the course of many days. The mean latency changed significantly between the training and treatment

days, but there was no collaboration between the preparation day and the groups, suggesting that differences between the groups were reliant on treatment. Results indicated that the zinc-based scaffold group at the concentration of 80 mg/kg via I/P injection displayed significant reduction of the escape latency time of animal as compared to the Streptozotocin-induced group (Figures 3–5). The drug at the same dose levels indicated significantly increased crossing number and north quadrant time spent in comparison with the Streptozotocin-induced group values. On both days, this group also displayed an upsurge in escape latency (Table 6).

Passive Avoidance Test (PAT). The retention latency time increased in all experimental groups except the Streptozotocin group, according to the findings. Following a 23 day chronic dosing schedule, these observations were gathered on the 24th day. When the findings of the zinc-based scaffold provided at different doses were compared to the first day training data, a significant increase in animal retention latency time was seen. Figure 6 displays the pattern of results at different doses of the testing compound.

Measurement of Biochemical Markers. The synthesized chemical moiety was found to have a prominent effect on the levels of biochemical markers. Levels of these endogenous antioxidants including CAT, SOD, and GSH were increased to a significant range ($P < 0.05$) inside the brain of animals that were treated with the zinc scaffold at the dose of 80 mg/kg in comparison with the Streptozotocin group. This synthesized chemical compound increased the endogenous antioxidant levels to a considerable amount that appeared above the normal level, while the control drug Streptozotocin gave a significant decline in antioxidant levels. When specifically considering the zinc carboxylate affecting MDA levels, it could not reach a significant level ($P > 0.05$) compared with the control Streptozotocin-treated group. The nitrile concentration appeared more interesting as it gave prominent results. The zinc scaffold at the dose regimen of 80 mg/kg gave significant values ($P < 0.05$), with decreased levels compared with the positive control Streptozotocin. Further in this case, interestingly, the zinc scaffold at the dose of 20 mg/kg gave the levels of nitrile as it appeared in the case of Piracetam-treated groups. All the values of biochemical markers are tabulated in Table 7. After treatment with the zinc scaffold, acetylcholinesterase levels seemed to be reduced, indicating larger amounts of acetylcholine neuro-

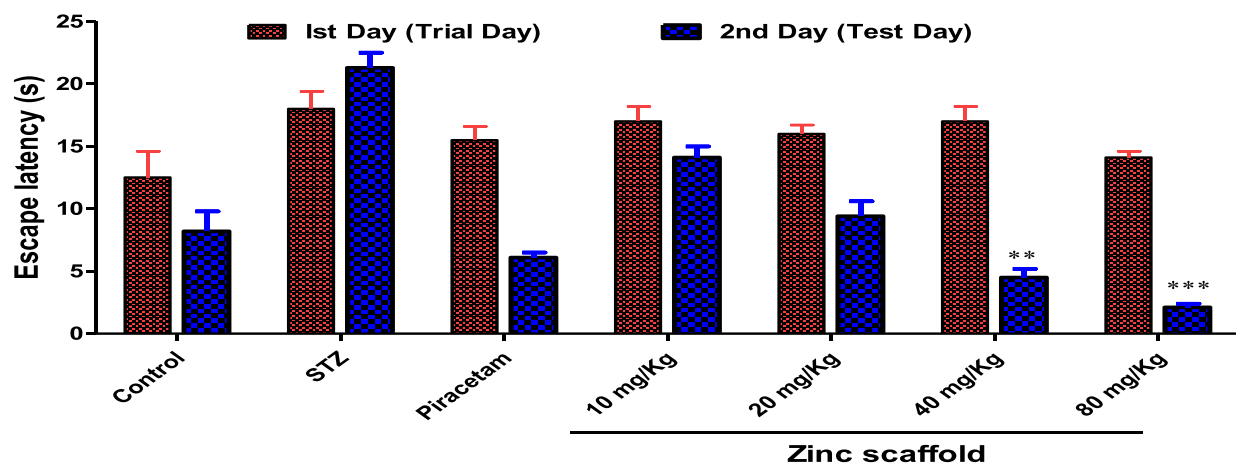


Figure 3. Effect of the zinc-based scaffold at altered dosage levels on escape latency (s) in the Morris water maze test. Representation of data as mean ± standard error of the mean; ** $P < 0.01$ and *** $P < 0.001$, $n = 10$, in comparison with first day and the Streptozotocin-treated groups.

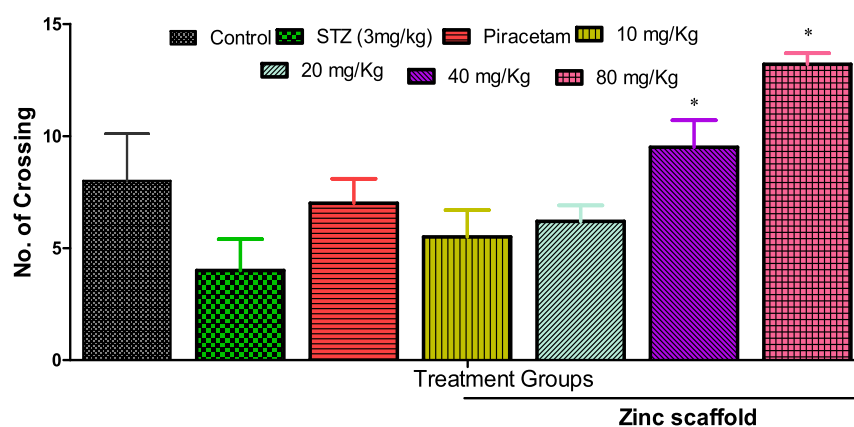


Figure 4. Outcomes of the zinc scaffold at altered dose levels on crossing numbers in the MWM test. Representation of data as mean \pm standard error of the mean; * $P < 0.05$, $n = 10$, in comparison with the Streptozotocin-induced group.

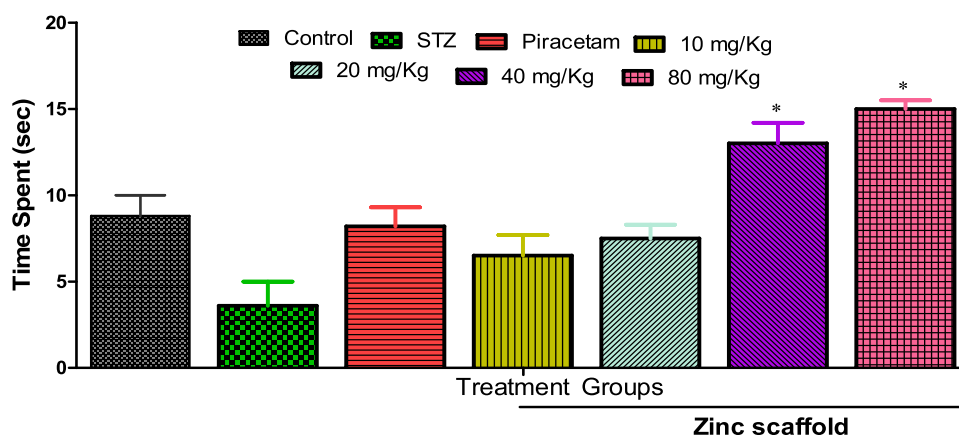


Figure 5. Effect of the zinc-based scaffold at changed dose levels on the period consumed (s) in the Morris water maze test. Representation of data as mean \pm standard error of the mean; * $P < 0.05$, $n = 10$, in comparison with the Streptozotocin-treated group.

Table 6. Time Spent in Open and Closed Arms of the Morris Water Maze Test^a

treatment group	time spent in open arm (s)	time spent in closed arm (s)
control	9.2 \pm 1.3	153 \pm 1.1
STZ	5.1 \pm 1.5 [#]	192 \pm 1.6 [#]
Piracetam (200 mg/kg)	8.8 \pm 0.7*	156 \pm 1.4*
zinc scaffold (10 mg/kg)	6.3 \pm 1.1*	173 \pm 0.3*
zinc scaffold (20 mg/kg)	7.5 \pm 0.2*	165 \pm 1.5*
zinc scaffold (40 mg/kg)	8.2 \pm 1.4*	143 \pm 1.4*
zinc scaffold (80 mg/kg)	9.5 \pm 0.9*	133 \pm 0.9*

^aRepresentation of data as mean \pm standard error of the mean; * $P < 0.05$, $n = 10$, compared with the Streptozotocin-treated group; [#] $P < 0.05$ vs control.

transmitters inside brain cells, which enhanced memory loss and forgetfulness.

Estimation of Neurotransmitters. After performing all the tests, it was estimated that the zinc scaffold at the dose regimen of 20, 40, and 80 mg/kg gave significant results ($P < 0.05$) with the increase in levels of dopamine, serotonin, and noradrenaline in comparison with the control group Streptozotocin. Research has shown that the upsurge in the levels of neurotransmitters is related to the improvement of short-term and long-term

memory and uplifting of the learning behavior with positive results. All the results are shown in Figure 7.

Computational Studies. To better understand the behavior of the synthesized chemical moiety when interacting with acetylcholinesterase and butyrylcholinesterase enzymes, computational studies were performed. The zinc scaffold gave excellent results by showing the binding energies of -8.8 and -8.5 kcal/mol for AChE and BChE, respectively. These binding energies showed that zinc-based ligands have the promising potential to behave as enzyme inhibitors. Figure 8 shows the three-dimensional and two-dimensional images of acetylcholinesterase interaction with the synthesized compound. It displayed one conventional hydrogen bond with Asp72 along with π - π stacked interaction with TrpA84 and Tyr121. Other important types of interactions were π -anion interaction with Asp72 and the carbon hydrogen bond with Gln69, Tyr70, and Asn85 with bond lengths of 3.41, 3.68, and 3.28 Å, respectively.

In analyzing the zinc scaffold interaction inside the butyrylcholinesterase enzyme, results are elaborated in Figure 9. The amide linkage inside the ligand gave excellent binding with Gly107 through a conventional hydrogen bond. Another hydrogen bond appeared with Tyr74 that interacted with the methoxy group, supporting the bonding energies. The π -sigma interaction was found with Val69 with a bond length of 4.91 Å. Other amino acid residues that appeared in the interaction included Ser78, Val83, Phe132, and Thr133 with bond lengths

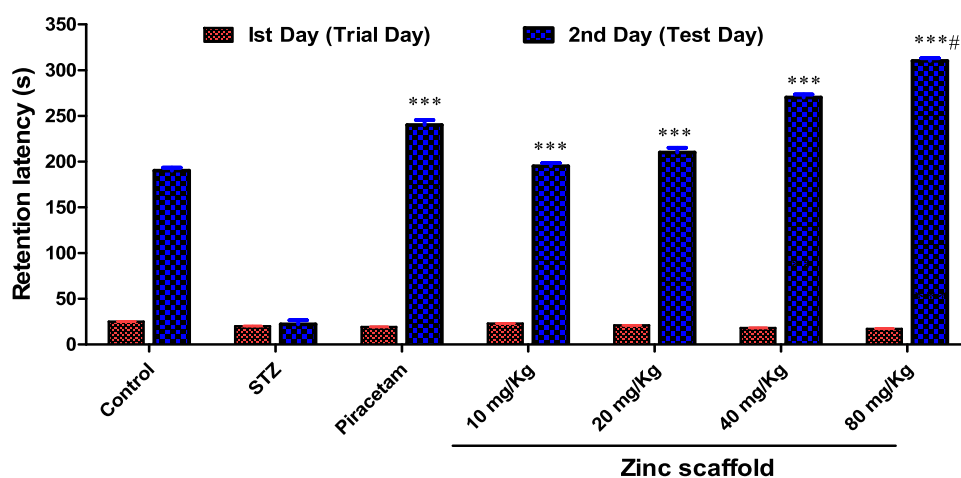


Figure 6. Representation of data as mean \pm standard error of the mean; *** $P < 0.001$, $n = 10$, in comparison with the Streptozotocin-treated group; # $P < 0.05$ in comparison to the control group.

Table 7. Levels of Biochemical Markers after Treatment with the Synthesized Zinc Scaffold^a

treatment group	GSH ($\mu\text{g}/\text{mg}$ of protein)	CAT ($\mu\text{mol}/\text{min}/\text{mg}$ of protein)	SOD ($\mu\text{g}/\text{mg}$ of protein)	MDA ($\mu\text{mol}/\text{mg}$ of protein)	nitrite ($\mu\text{g}/\text{mg}$ of protein)	protein ($\mu\text{g}/\text{mg}$ of protein)	AChE ($\mu\text{mol}/\text{min}/\text{mg}$ of protein)
control	25 \pm 0.3	152 \pm 0.3	44 \pm 0.3	0.17 \pm 0.6	3.5 \pm 0.05	462 \pm 0.6	1.7 \pm 0.02
Streptozotocin	19 \pm 0.05 [#]	98 \pm 0.5 [#]	25 \pm 0.4 [#]	0.23 \pm 0.3 [#]	4.6 \pm 0.03 [#]	392 \pm 1.5 [#]	2.5 \pm 0.4 [#]
Piracetam (200 mg/kg)	21 \pm 0.3 [*]	116 \pm 0.3 [*]	42 \pm 0.3 [*]	0.18 \pm 1.4 [*]	3.5 \pm 0.05 [*]	465 \pm 1.2 [*]	1.6 \pm 0.5 [*]
zinc scaffold (10 mg/kg)	20 \pm 0.5	109 \pm 0.7 [*]	29 \pm 0.1 [*]	0.38 \pm 0.6 ^{#,α}	3.7 \pm 0.08 [*]	444 \pm 0.6 [*]	1.8 \pm 0.3 [*]
zinc scaffold (20 mg/kg)	25 \pm 0.1 [*]	117 \pm 0.4 [*]	36 \pm 0.4 [*]	0.36 \pm 0.3 ^{#,α}	3.5 \pm 0.03 [*]	482 \pm 2 [*]	1.7 \pm 0.04 [*]
zinc scaffold (40 mg/kg)	26 \pm 0.07 [*]	123 \pm 0.6 [*]	39 \pm 0.1 [*]	0.37 \pm 0.3 ^{*,#,α}	3.4 \pm 0.05 [*]	628 \pm 2.3 ^{*,#,α}	1.3 \pm 0.1 [*]
zinc scaffold (80 mg/kg)	27 \pm 0.02 ^{*,α}	127 \pm 0.08 ^{*,α}	42 \pm 0.2 [*]	0.37 \pm 1.2 ^{*,α}	3.2 \pm 0.04 [*]	658 \pm 2 ^{*,#,α}	0.7 \pm 0.05 ^{*,α}

^aData are presented as mean \pm SEM, $n = 10$; * $P < 0.05$ was given compared with the Streptozotocin-treated group; # $P < 0.05$ vs control; ^α $P < 0.05$ vs positive control.

of 3.13, 5.46, 5.44, and 3.32 Å, respectively. The two-dimensional visualization is shown in Figure 9.

Protein Analysis by ELISA. Enzyme-linked immunosorbent assays were utilized to determine the behavior of the synthesized zinc scaffold against the tau proteins and amyloid- β proteins. These were performed through specific ELISA kits, which showed that the synthesized chemical moiety at the dose regimen of 20, 40, and 80 mg/kg decreases the levels of these proteins within the brain cells of testing animal models, which in turn increases the cognitive behavior and activities of experimental animals (Figure 10).

Histopathological Studies. Histopathological studies involve the study and diagnosis of diseases at the tissue level involving examination through microscopic parameters. They are liable for making tissue diagnosis and treatment of patients at the tissue level. When the zinc-based scaffold chemical moiety was studied at histopathological levels, it was indicated that this compound displayed a minute change at a lower dose of 20 mg/kg, while increasing the dose led to an increase in protective effects through decreased neurodegeneration and the number of unhurt cells in line. The comparison of the testing drug was made with the positive control Piracetam that promoted the cognitive behavior and enhanced the acetylcholine neurotransmitter levels. The results of these pathological studies are elaborated in Figure 11.

AChE Analysis through RT-PCR. The zinc-based scaffold has a prominent role in the reduction of the acetylcholinesterase level, which in turn increases the level of acetylcholine. This was notified through the mRNA expression of acetylcholinesterase that declined up to 1.45 \pm 0.33 at the dose of 40 mg/kg in comparison with that of the disease control Streptozotocin-induced group (2.85 \pm 0.16). The primers that were involved in acetylcholinesterase analysis are listed in Table 8. This reduction was increased with the increase in the dose of the testing chemical moiety, which indicated that this compound has a prolonged effect with the increase in concentration in a dose-dependent manner. Results are elaborated in Figure 12.

DISCUSSION

Alzheimer's disease (AD) is a cumulative neurodeteriorating illness that is associated with the advanced stage of dementia.^{2,21} It initially involves behavioral fluctuations, cognitive dysfunctions, emotional variation, and sleep abnormalities, which later move to advancements like organ failure, malnutrition, necrosis, and ultimately, neuronal cell death.³ For induction of Alzheimer's disease in experimental animals, a persistent dose of Streptozotocin was injected through the intracerebroventricular route, which results in the impairment of metabolic activities and malfunctioning of the brain due to the increase in oxidative stress.⁵ Ultimately, due to these parameters, adenosine

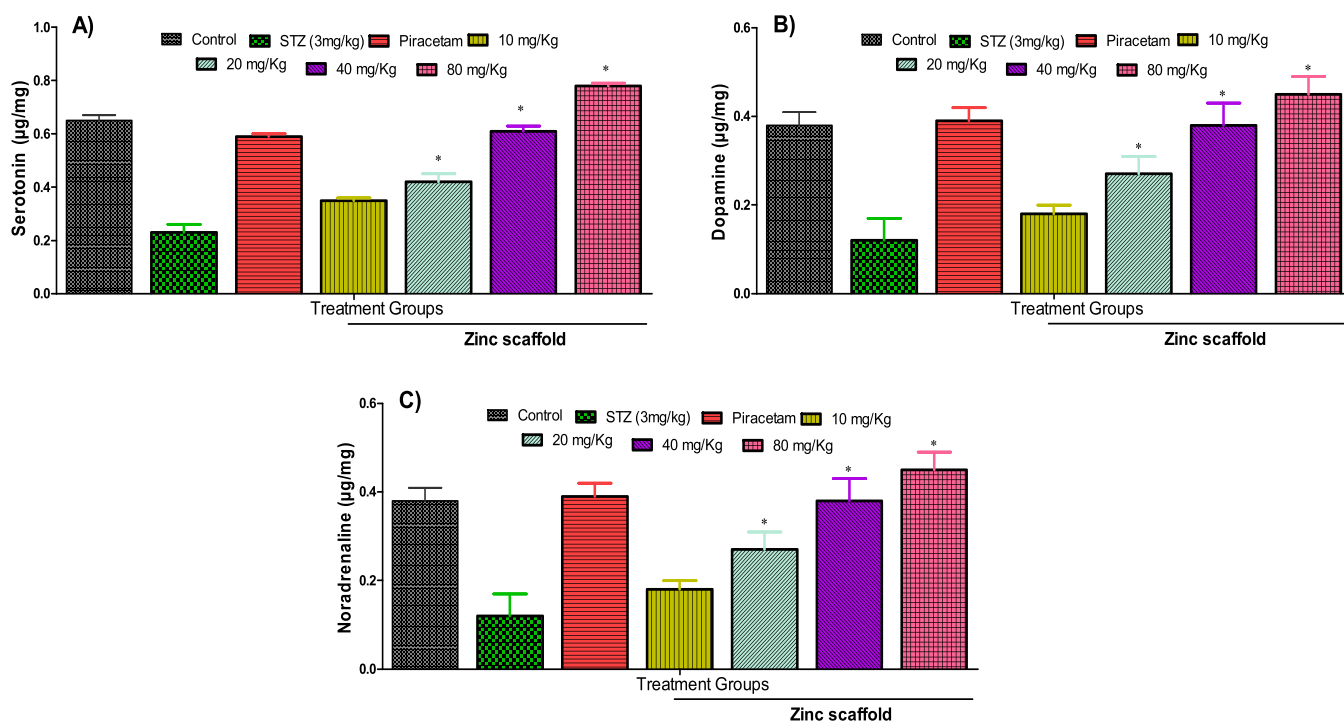


Figure 7. Effect of the zinc scaffold in mouse brain neurotransmitter levels. Representation of data as mean \pm standard error of the mean; * $P < 0.05$, as compared with the Streptozotocin-treated group. (A) Serotonin, (B) dopamine, and (C) noradrenaline.

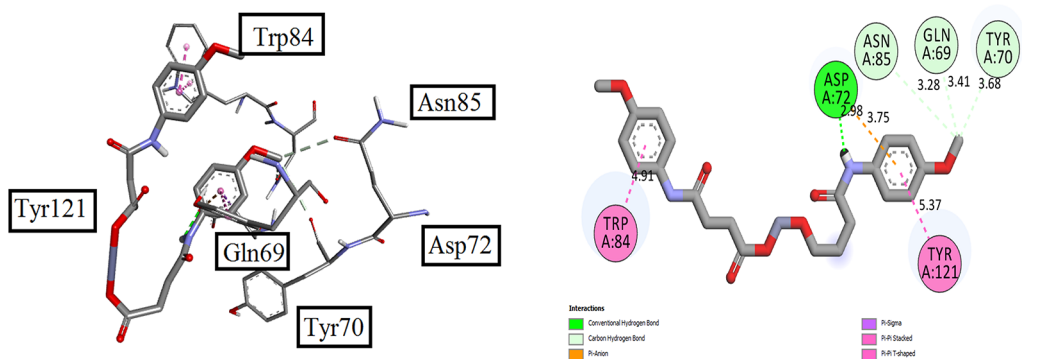


Figure 8. 3D and 2D images of the synthesized compound with the acetylcholinesterase enzyme.

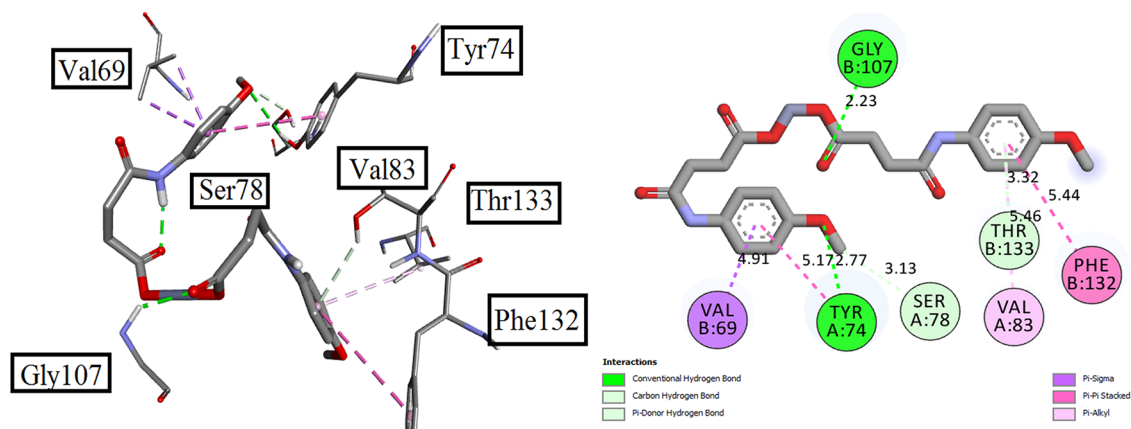


Figure 9. 3D and 2D images of the synthesized compound with the butyrylcholinesterase enzyme.

triphosphate levels decrease, causing cholinergic deficits inside the brain cells. Furthermore, this decrease in adenosine triphosphate levels increases the formation of reactive oxidative

species, deposition of amyloid- β plaques, the release of mediators of inflammation, and deposition of neurofibrillary tangle phosphorylated proteins inside brain cells.⁶ Accumulation

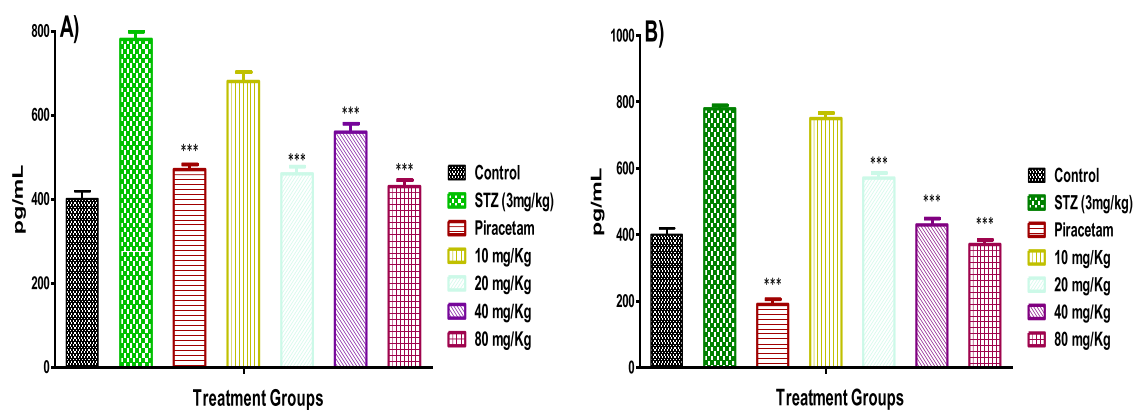


Figure 10. The amounts of (A) amyloid- β and (B) tau proteins in the brains of mice were calculated. In comparison to the STZ-treated group, $***P < 0.001$ was given in comparison to STZ treated group.

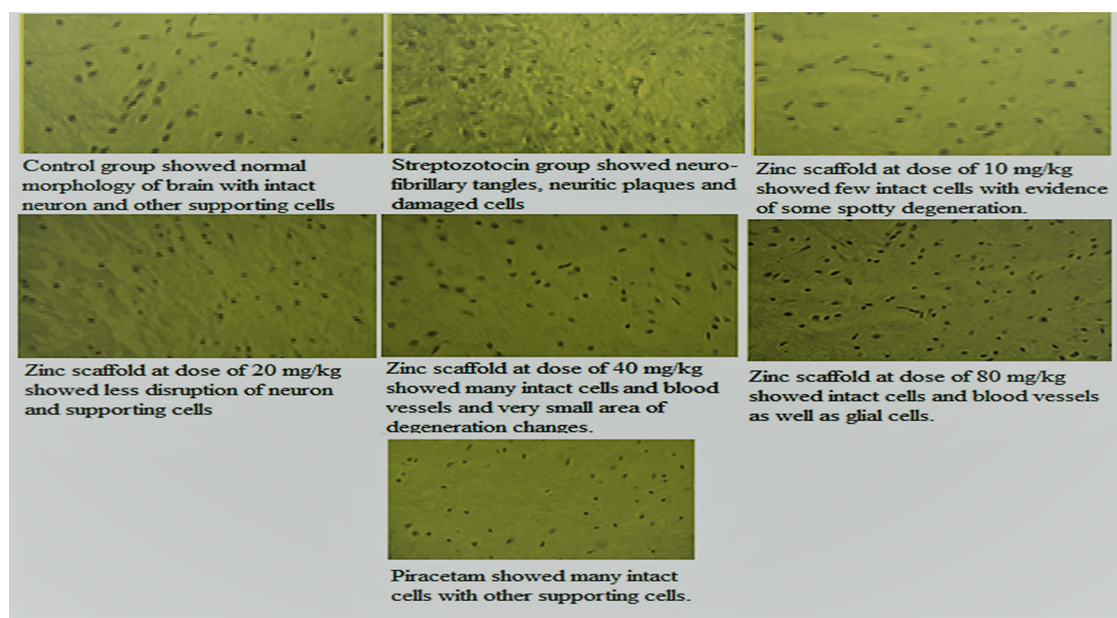


Figure 11. Histopathological characteristics of zinc scaffold-, Piracetam-, and Streptozotocin-treated groups.

Table 8. List of Primers Utilized in RT-PCR

primer	primer sequence
acetylcholinesterase	forward sequence: A G G A C G A G G G C T C C T A C T T T reverse sequence: C A R G G C A T C T C T C A G G T G G G
GADPH (glyceraldehyde dehydrogenase 3-phosphate)	forward sequence: G G A G T C C C C A T C C C A A C T C A reverse sequence: G C C A T A A C C C C A C A A C A C

of oligomers is also harmful to cells especially in the brain of an Alzheimer's disease patient where they penetrate the cell membrane, initiating a series of pathological reactions ending in cell death. Due to these reasons, the scrutinizing of new molecule effects in memory impairment is important. Organometallic compounds are always a point of attraction for researchers as they provide a more realistic approach for scientists to discover new drugs.⁸ Zinc is one of trace elements that, in minute quantities, provide effective pharmacological effects. It is involved in anticancerous, anti-ulcer, anti-inflammatory, antimicrobial, antifungal, antileishmanial, and other important biological activities. The synthesized compound zinc scaffold was tested via *in vitro* test and proved to be effective compared with standard positive controls.¹⁰ Molecular docking studies were employed through AutoDock Vina

interlinked with PyRx software that provides binding affinities inside the active site and binding pocket of targeted proteins.²⁶ This synthesized chemical moiety was tested for behavioral assessment through animal models that were designed for Alzheimer's disease. An open field test was first conducted to examine the locomotor activity of the tested animals as well as their anxiolytic and exploratory responses.²⁹ In comparison to the Streptozotocin group, the results from the open field test showed that the zinc scaffold at the greatest level of dose, 80 mg/kg, increased anxiolytic behavior and exploration with greater locomotor activity. Anxiety has been linked to a reduction in cognitive reserve in studies. There was a link between anxiolytic activity and a drop in cognitive expression according to these research studies. Anxiety, according to some research, is the outcome of oxidative stress damage and inflammation in the

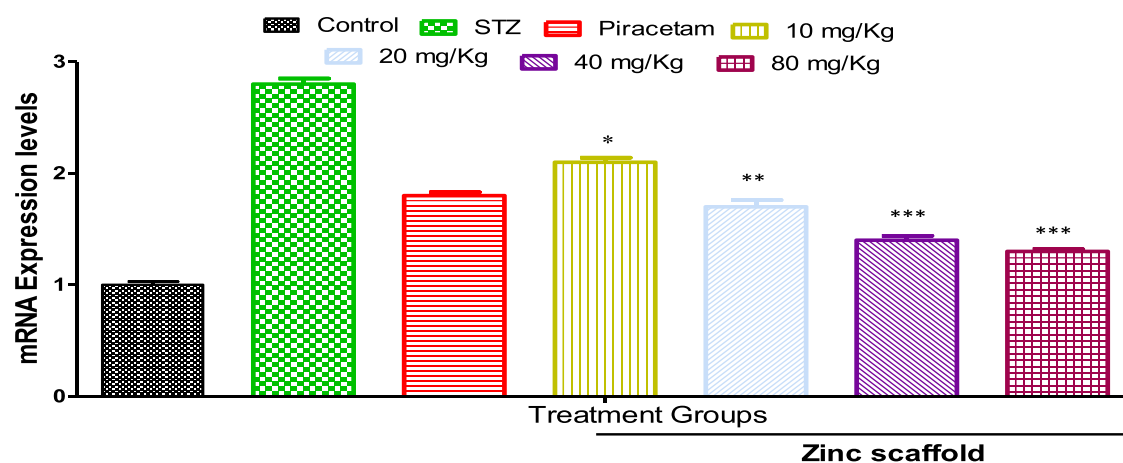


Figure 12. Representation of data as mean \pm standard error of the mean; * $P < 0.05$, ** $P < 0.01$, and *** $P < 0.001$ were given in comparison to the Streptozotocin group.

central nervous system.¹² Neuronal death to cells due to oxidative stress and neuronal dysfunction provoked by Alzheimer's disease-linked $A\beta$ proteins gave a major contribution toward the pathogenesis of this neurodegenerative disorder.¹³ Therefore, prevention of antioxidant-based detrimental free radical consequences gave an important neuroprotective approach. Although there has been multiple experimental evidence about the neuroprotective potential of antioxidants, the clinical justifications about the protective behavior are still a dilemma. The free radical scavenging potential of natural and synthesized compounds constitutes an important consideration for the treatment of Alzheimer's disease.²² Two-directional association between anxiety and amyloid plaques leads to changes in the behavior of test models.²² Increased anxiety in persons with $A\beta$ plaques gave an immediate decrease in the cognitive routine. Animals that spent more time in the center area had lower anxiety levels than those that spent less time there.²³ One of the behavioral evaluation tests, the raised plus maze test, resulted in a higher anxiety score. It was further demonstrated by a drop in entry counting and a decrease in time spared in an open arm, both of which imply anxiety levels. In comparison to the Streptozotocin group, the zinc carboxylate scaffold showed extremely significant data such as a $P < 0.001$ decrease in latency transfer and a $P < 0.05$ increase in the counting of open arm entries and time spared in open arms at 80 mg/kg dosing regimen.²⁶ Using a water maze test, the effect of the synthesized chemical moiety on spatial memory was investigated. This exam was used to assess spatial learning. It belongs to the best established model for the assessment of memory and learning. In contrast to day one and medication-induced illness groups, the zinc scaffold at a dose level of 80 mg/kg significantly ($P < 0.05$) demonstrated that the enhanced quantity of crossovers and additional time spared in the targeted north quadrant, as well as escape latency, dramatically declined ($P < 0.001$). The step-down passive avoidance test was used to estimate long-term memory based on the sort of learning that was employed to prevent step-down behavior in order to avoid punishment. In comparison to the first day and Streptozotocin-treated groups, zinc carboxylate at 80 mg/kg dosage resulted in a significant ($P < 0.001$) increase in retention delay.

At 80 mg/kg dosage, the levels of catalase, glutathione, superoxide dismutase, and proteins were considerably increased.³⁵ As a result, there is a drop in nitrite levels, which indicates a reduction in oxidative stress, which leads to improved

memory. At all zinc scaffold doses, the quantity of malondialdehyde, a lipid peroxidation indicator, rose. Acetylcholinesterase levels were significantly ($P < 0.05$) and dependently reduced with this synthesized zinc scaffold, and the decrease in acetylcholinesterase levels could be attributed to the indirect cholinergic effect of the zinc scaffold, which leads to an increase in acetylcholine levels by inhibiting acetylcholinesterase.²⁷ The effect of the zinc-based chemical moiety on memory improvement could be through the acetylcholine binding to the nicotinic receptors nAChRs inside brain cells, which raises the cytoplasmic levels of calcium and stimulates the intracellular calcium-dependent processes like gene expression and neurotransmitter release that were linked to the improvisation of memory and also learning improvement. The mechanism by which the zinc scaffold inhibits the acetylcholinesterase activity was further elaborated by *in silico* molecular docking studies.²⁶ By forming the ligand–receptor interaction complex and modeling conformations, these computational studies provide the understanding of the behavior of drug modulation. The molecular docking strategies are simulation-based strategies that account for the structural reorganization of movable side chains and residues at the receptor's active site upon ligand binding, as well as precise ligand placement into the receptor's binding site to avoid false positive results due to receptor flexibility. The zinc scaffold was shown to have a higher binding affinity for acetylcholinesterase than the standard, suggesting that the experimental suppression of acetylcholinesterase was effective. The hydrophobic and hydrophilic interactions of the zinc chemical moiety with a range of key amino acid residues that are critical for acetylcholinesterase activity justify its higher binding affinity.²⁵ The majority of Piracetam anticholinesterase activity-preserving residues were involved in a variety of zinc chemical moiety-interacting residues, although the form of bonding was varied. As a result, the chemical compound's higher binding affinity for acetylcholinesterase, as well as its diverse contacts and bonding pattern, may support its experimental inhibition of acetylcholinesterase over Piracetam. The levels of neurotransmitters such as noradrenaline and serotonin were shown to be lower when Streptozotocin was injected intracerebroventricularly in one of the scientist's prior studies.²⁹ A dip in brain glucose levels and energy expenditure might be the cause of the decrease in neurotransmitter titer. People with Alzheimer's illness showed reduced levels of noradrenaline, serotonin, and 5-HT according

to another study. The protein kinase or cyclic adenosine monophosphate noradrenaline triggered the activation of a circuit. Compared to the Streptozotocin group, the zinc scaffold at an 80 mg/kg dosing schedule resulted in a substantial $P < 0.05$ increase in dopamine, serotonin, and noradrenaline levels.³¹ Zinc compounds have been discovered to boost the amount of cyclic adenosine monophosphate, adenosine triphosphate, and cyclic adenosine monophosphate in the presence of an adenylyl cyclase enzyme, resulting in the creation of cyclic adenosine monophosphate.³² The cyclic AMP activates protein kinase A, which phosphorylates the cAMP response element binding protein CREB. Memory improvement has been implemented in this way.

MATERIAL AND METHODS

Chemicals. Phosphate buffer saline (PBS), DPPH, ABTS, hydrogen peroxide (H_2O_2), toluene, pyridine, Piracetam (GlaxoSmithKline), Streptozotocin, sodium hydroxide, acetylcholinesterase, butyrylcholinesterase enzymes, dopamine, and noradrenaline were purchased from Sigma-Aldrich and utilized without further purification. Magnesium chloride, dextrose, monobasic sodium phosphate, and monobasic potassium phosphate were purchased in purified form through Riedel-de Haen, United States. The synthesized chemical moiety was obtained from the King's College London, School of Cancer and Pharmaceutical Sciences, United Kingdom, after the complete spectroscopic analysis and confirmation of the structure. The structure of the synthesized compound is given in Figure 1.

EXPERIMENTAL ANIMALS

Male and female fully grown Swiss albino mice, with a weight of 25–40 g and aged 6–8 weeks, were obtained from the Department of Pharmacy, University of Malakand, Chakdara, Lower Dir, Pakistan. These experimental animals were kept for 12 h in light and 12 h in the dark under standardized conditions with the temperature maintained at 25 ± 1 °C and moisture of 40–50%. Experimental procedures were carried out during 4 am to 8 pm. These albino mice were permitted free access to their food and water.²³

Approval by the Ethical Committee. All the animals and protocols for the experimental design were implemented after the approval from the ethics committee of the Pharmacy Department, University of Malakand, Chakdara, Lower Dir, KPK. Testing animals were kept under light and humidity conditions that were approved by the ethical committee with the number UOM/REC/2022/041.²⁴

Experimental Grouping of Animals. The experimental animals were split up into seven groups with 10 mice in each. Group I: vehicle control group receiving carboxyl methyl cellulose (CMC), i.e., 1 mL/100 g intraperitoneally; group II: group receiving 3 mg/kg Streptozotocin (STZ) intraperitoneally; group III: positive control group receiving 200 mg/kg Piracetam intraperitoneally; group IV: 10 mg/kg zinc scaffold intraperitoneally; group V: 20 mg/kg zinc scaffold intraperitoneally; group VI: 40 mg/kg zinc scaffold intraperitoneally; group VII: 80 mg/kg zinc scaffold intraperitoneally. Except for the control group, all groups received 3 mg/kg Streptozotocin (STZ) via intracerebroventricular injection unilaterally on the first and third days of this experiment by utilizing a stereotaxic device apparatus. Until the 23rd day of the treatment regimen, all groups received their respective doses, which were designed on the basis of human dosing by the conversion formula. Doses

to the animals were given according to the weight of animals. Signs of morbidity and mortality were tested and verified on the daily basis.

In Vitro Assays. Acetylcholinesterase Assay. Ellman's experiment was used to investigate the enzyme inhibitory activity of substances using acetylcholinesterase extracted from electric eel and butyrylcholinesterase separated from equine serum. This procedure depends upon the formation of the 5-thio-2-nitrobenzoate anionic radical. Results were finalized by the formation of a yellowish color due to 5,5-dithio-bis-nitrobenzoic acid. After all the procedures, the samples were analyzed through spectroscopic analysis at 412 nm. The positive control was selected as Galantamine, which provided acetylcholinesterase and butyrylcholinesterase enzyme inhibition at the maximum level.²⁵

DPPH Radical Scavenging Assay. All the synthesized compounds were tested for the free radical scavenging activity using the free radical DPPH scavenging potential using the DPPH method as in reported research works. Various synthesized compound dilutions were poured to the 0.004% methanolic solution of DPPH. The absorbance was measured at 517 nm using a UV spectrophotometer after 30 min.²⁶

ABTS Free Radical Scavenging Assay. The antioxidant capacity of the testing sample was investigated using ABTS free radical scavenging assay.²⁷ This assay is based on the ability of antioxidants to scavenge ABTS radical cations, which results in a decrease in IR absorbance at 734 nm.

Hydrogen Peroxide Scavenging Assay. The H_2O_2 scavenging activity of the sample was determined using the method described previously in reported procedures. The absorbance was measured at 230 nm.²⁸

Acute Toxicity Test. Acute toxicity test was performed to evaluate possible toxicity at higher doses. Effects were monitored for first 4 h, and then mortality was observed after 24 h.²⁹

In Vivo Studies. Following the administration of test samples, behavioral tests were carried out to determine locomotor activity (exploratory behavior) such as grooming and raising of the animals.³⁰

Behavioral Assessments. Open Field Test. The apparatus open field that consisted of an area of 40×40 cm with a height of 36 cm was used for the testing of locomotor and exploratory behavior.³¹ The square area of this apparatus has 16 squares, centralized by 4 subsquares highlighted with color green. At the start of the test, the mouse was placed in it and was observed for 300 s. The mouse right away moved toward the boundary highlighted as red, and the period to move from the midpoint to margins was noted down. This time is called latency time. In this examination, the number of interchanges and the period spent from the midpoint to the boundary were recorded. Other measurements observed in this test were brought up, i.e., jumping and movements made by an individual mouse to the gateway were perceived.³²

Elevated Plus Maze Test (EPMT). An elevated plus maze apparatus consists of two $25 \times 5 \times 0.5$ cm open arms diagonal to each other and two $25 \times 5 \times 16$ cm closed arms. Open arms are perpendicular to closed arms with a $5 \times 5 \times 0.5$ cm center platform. The elevation of the apparatus was 50 cm from the floor. This test was carried out at the end of second week of treatments. The response of the mouse was noted for 5 min. The mouse was positioned at one of the open arm ends facing toward the central side, and the latency time was calculated. This time period accounted for the duration it took to enter in any of the

closed arm within 1.5 min. Furthermore, the retention of memory was observed within 1 day. The time spent by the mouse and the amount of accesses in any of the arms were also noted in this test.³³

Morris Water Maze (MWM) Test. This test was used to assess the mental representation of an animal with its environment and for spatial memory.³⁴ The main component of this setup is a round pool, about 6 feet in width and 3 feet in depth. The pool was filled with water that was made cloudy with powdered nonfat milk with a temperature maintained at 23 ± 1 °C. This setup consists of north, south, east, and west quadrants. A platform that is 10 cm in diameter was placed in the center of any quadrant so that the test animal can stay on that platform.²¹ The test was carried out during 15th to 19th drug treatment days. All test animals were trained so that they could allocate the probe and practice to stay on it for half a minute after finding the position of the probe within 1 min. After all training sessions, the Morris water maze test was performed without a platform and animals were observed for 3 min. The escape latency time was measured for each of the testing animal.³⁵

Passive Avoidance Test. This test was used to analyze the cognitive behavior of the mouse. This test measures the basic ability of an animal to learn and memorize the presence of a stimulus. This apparatus has a wooden platform with a dual compartment; one is white, while the other is dark. Animals were placed in a white compartment, and doors were opened for assessment in the dark compartment. The time period to enter the dark compartment was recorded. When the animal entered the dark area, doors were allowed to close and an electric shock of 1–2 s was given (0.2–0.5 mA). On the result day, the time was noted when the animal entered the dark compartment with all its four paws. This time was called the retention latency, and an increase in retention latency was the indicator of the memory retention and cognitive improvement.³⁶

Measurement of Biochemical Parameters. Brain Homogenate Preparation. On the 24th day of treatments, all treated animals were anesthetized with 3–5% isoflurane diluted in oxygen. Animals were sacrificed by cervical dislocation, and the brain was extracted and washed with NaCl (0.9%). Tissue homogenates were prepared in 0.1 M phosphate buffer having pH 7.4 with 1/10 ratio. This homogenate was centrifuged at 6000 rpm at 4 °C for 10 min. The supernatant was collected for further biochemical and ELISA assays.

Estimation of the Glutathione Level. In 1 mL of supernatant, 10% trichloroacetic acid (1 mL) was added to precipitate the protein, and 4 mL of phosphate solution and 0.5 mL of 5,5-dithiobis-2-nitrobenzoic acid (DTNB) were added to the supernatant. The absorbance was observed at 412 nm. The glutathione level was estimated as $\mu\text{g}/\text{mg}$ of protein by using the following formula:

$$\text{glutathione level} = X - 0.00314/0.0314 \times D(f) \div B(t) \times V(a)$$

where X represents the absorbance at 412 nm, $D(f)$ is the dilution factor, $B(t)$ represents the homogenate of brain tissue, and $V(a)$ is the aliquot volume, i.e., 1 mL.³⁷

Catalase Activity Measurement. The supernatant (0.05 mL) of tissue homogenate and phosphate buffer with pH 7.0 (1.95 mL) were added and mixed well. One milliliter of 30 mM hydrogen peroxide was poured to the mixture, and the alteration in absorbance was measured at 240 nm. The values were observed as μmol of hydrogen peroxide per milligram of protein

per minute. This activity was calculated through the following formula:

$$CA = O. D. / E \times V \times \text{protein (mg)}$$

where CA represents the catalase activity, O.D. represents the change in absorbance every minute, and E represents the extinction coefficient of H_2O_2 ($0.071 \text{ mmol}^4/\text{cm}$).³⁸

Superoxide Dismutase (SOD) Estimation. In this method, 0.1 M potassium phosphate buffer with pH 7.4 (2.8 mL), tissue homogenate (0.1 mL), and pyrogallol (0.1 mL) were mixed thoroughly. This pyrogallol is one of the known oxidizing agents that were used to work under alkaline conditions with generation of oxygen. Superoxide dismutase quickly reduced the oxygen to superoxide anionic radicals.³⁹ The resultant mixture absorbance was recorded at 325 nm using a UV spectrophotometer. The superoxide dismutase level was estimated through the slope equation $Y = 0.0095X + 0.1939$.

Malondialdehyde Activity (MDA) Estimations. In 1 mL of supernatant, 1 mL of thiobarbituric acid (4 mM) was added. This mixture was cooled on an ice bath for 15 min. After cooling, the mixture was centrifuged at 3500 rpm for 10–12 min. The absorbance was measured at 532 nm after collection of the supernatant with final results elaborated in $\mu\text{mol}/\text{mg}$.³⁹ Final calculations were performed through the following equation:

$\text{MDA concentration} = \text{Abs}(532) \times 100 \times V(t)/163.8 \times W(t) \times V(u)$ where $\text{Abs}(532)$ represents the absorbance at 532 nm, $V(t)$ indicate the 4 mL mixture volume, 163.8 indicates the molar coefficient, $W(t)$ indicates the weight of the dissected brain, and $V(u)$ indicates the 1 mL bulk of aliquot.

Nitrile Level Estimation. Considering the calculations of all parameters, the level of nitrile was confirmed by the Griess reagent. The procedure involves the mixing of brain homogenate and Griess reagent in an equal concentration with an incubation period of 10 min. Absorbance of the reaction mixture was observed at 546 nm. Following the regression equation of slope, the nitrile levels were estimated as $Y = 0.003432X + 0.0366$.⁴⁰

Protein Content Evaluation. To perform this procedure, three solutions were prepared and designated as solution A, solution B, and solution C. Solution A was prepared by taking 2% Na_2CO_3 in 0.1 N of NaOH. Solution B consists of 1% sodium potassium tartrate in water, and solution C involves 0.5% copper sulfate in water. Afterward, two reagents were prepared. Reagent 1 contains solution A (48 mL), solution B (1 mL), and solution C (1 mL), while reagent 2 consists of Folin-phenol reagent and water with a ratio of 2:1. Determination of protein contents was carried out by addition of 0.2 mL of tissue homogenate to 4.5 mL of reagent 1 followed by incubation for 10 min with addition of 0.5 mL of reagent 2 with re-incubation for 30 min.⁴¹ Final calculations were carried out through absorbance measurement at 660 nm with the slope of regression line as $Y = 0.0000757X + 0.0000476$.

Acetylcholinesterase Activity Estimation. This assay was performed to determine the acetylcholinesterase activity. Tissue homogenate (0.4 mL) was poured in 2.6 mL of 0.1 M solution of phosphate buffer with pH 8 along with 100 μL of DTNB followed by absorbance observation at 412 nm. Within this solution, 20 μL of acetylcholine iodide was poured and the absorbance was observed again at 2 min interval for 10 min.⁴² The deviation in absorbance was calculated through the formula $R = 0.000574 \times \Delta A/\text{co}$, where R indicates the rate, i.e., substrate moles hydrolyzed per minute, ΔA indicates the absorbance

change per min, and *co* represents mg/mL of the real concentration of the tissue expressed.

Estimation of Neurotransmitters. Aqueous Phase Preparation. Five milliliters of HCl-butanol-containing homogenate was prepared and centrifuged for 20 min at 2000 rpm. Heptane (2.5 mL) along with 0.31 mL of 0.1 M HCl was added and recentrifuged for 10 min in two phases. Experimentation was performed at 0 °C. One phase containing the organic portion was wasted, and 0.2 mL of the watery phase was utilized to estimate the level of serotonin, dopamine, and noradrenaline.

Serotonin Level Estimation. For the estimation of serotonin, 0.25 mL of *o*-phthaldialdehyde (OPT) and 0.2 mL of homogenate were mixed and heated for 10 min at 100 °C. The absorbance was observed at 440 nm after the temperature of the sample reached the ambient level. For the blank, 0.25 mL of HCl was added without the OPT. The serotonin level was analyzed by utilizing the serotonin regression of the line equation.⁴³

Estimation of Dopamine and Noradrenaline Levels. To estimate the levels of dopamine and noradrenaline, the following procedure was carried out. HCl (0.05 mL, 0.4 M) was added to 0.2 mL of watery phase of tissue homogenate with 0.1 mL of ethylene diamine tetraacetic acid (EDTA) and sodium acetate. Afterward, 0.1 mL of 0.1 M iodine solution in ethanol was poured to oxidize the mixture. This oxidation reaction was turned off with addition of 0.1 mL of sodium sulfate followed by the addition of 0.1 mL of acetic acid and heating at 100 °C for 6 min. The sample was permitted to cool down, and the absorbance was estimated at 350 and 450 nm for dopamine and noradrenaline, respectively.³⁹ To perform the reverse-order oxidation, the blank was synthesized by adding reagents, i.e., sodium sulfate before iodine solution. Final calculations were carried out using the following regression line equations: for dopamine, $Y = 0.2331X + 0.0164$, and for noradrenaline, $Y = 0.1008X + 0.2508$.

■ COMPUTATIONAL STUDIES

Molecular docking MD studies were performed to investigate the binding affinities of the zinc-based scaffold with acetylcholinesterase (AChE) and butyrylcholinesterase (BChE) enzymes utilizing AutoDock Vina 1.2. interlinked with PyRx software, which has the authenticity to perform the computational studies. The three-dimensional models of proteins of acetylcholinesterase and butyrylcholinesterase were downloaded from the Protein Data Bank (<https://www.rcsb.org>) as 1EVE and 1POI, respectively, and saved in PDB format. Modification of these protein models was performed through removal of cocrystallized ligands and water of crystallization. The synthesized chemical moiety zinc scaffold was sketched in ChemDraw 20.0 software and saved as a MOL file. This saved file was reopened in Discovery Studio Visualizer Bio Via, and modification of structures was performed and saved in PDB format. At this stage, both the structure of proteins and synthesized chemical moiety were ready to be docked, which was performed in AutoDock Vina. The grid box was selected, and the docking procedure was performed. Results were elaborated in Discovery Studio Visualizer and further explained through Pymol and Ligplot software.⁴⁴

■ PROTEIN ANALYSIS BY ELISA

The analysis of proteins was carried out by using ELISA kits for estimation of amyloid- β and tau proteins. These 1–40 A β and

tau proteins in complexation with HRP conjugates were added along with TBM solution. The reaction was stopped with the help of a stop solution. A color change was noticed at 450 nm.³⁹ Protein levels were estimated by the standard curve. 1–40 A β amyloid levels (pg/mL) were observed through the following mentioned regression line $Y = 0.00397X + 0.1504$, and the tau protein levels were estimated using $Y = 0.0008508X + 0.7008$.

■ HISTOPATHOLOGICAL STUDIES

After performing the behavioral assessments and other experimental steps, animals were sacrificed and brain tissue was preserved in 10% formaldehyde solution. Brain tissue fixation was performed in wax blocks, and tissue sections were cut at 40 μ m utilizing a digital microtome. Olmos stain was used to identify the color at 100 \times magnifying power after cutting the brain sections.⁴⁵

■ ACHE ANALYSIS THROUGH RT-PCR

For PCR analysis, the brain tissues were treated with triazole solution and RNA was extracted. For RNA transcription to cyclic DNA, a reverse transcription kit was used. Afterward, polymerase chain reaction studies were performed under the conditions that the procedure was done at 95 °C for 300 s along with 40 cycles with a moderate 60 °C temperature, which was varied further for 20 s to 72 °C. The expression of mRNA of acetylcholinesterase was identified by the internal control GAPDH and PCR.⁴⁶

■ STATISTICAL ANALYSIS

GraphPad Prism software version 5 was used to perform statistical analysis. Every value was taken as triplicate and represented as mean \pm standard error of the mean. Values were taken as a probability with * $P < 0.05$ as mildly significant levels, ** $P < 0.01$ as moderately significant levels, and *** $P < 0.001$ as highly significant levels.

■ CONCLUSIONS

This research was carried out to analyze the zinc-based scaffold as a neuroprotective agent. This research work was concluded with the outcome that the zinc scaffold improved the memory impairment in a dose-dependent manner. After *in vitro* assessment of this synthesized chemical moiety for the acetylcholinesterase enzyme inhibition potential, DPPH, ABTS, H₂O₂ free radical scavenging potential, and acute toxicity test, *in vivo* activities were performed. Behavioral assessments include open field test, elevated plus maze test, Morris water maze test, and passive avoidance test, which showed the improved leaning behavior of testing animals after administration of the zinc derivative. Furthermore, estimation of biochemical parameters was carried out including brain homogenate formation, glutathione level estimation, catalase activity estimation, superoxide dismutase estimation, malondialdehyde activity, nitrile level estimation, and protein content evaluation. Neurotransmitter levels including serotonin, dopamine, and noradrenaline levels were also analyzed after zinc derivative estimation. Docking studies were performed, which displayed the improved interaction of the synthesized chemical moiety at the binding site of acetylcholinesterase and butyrylcholinesterase enzyme. Protein analysis through ELISA and histopathological studies also supported the results. This research ended up with the results that the zinc scaffold improved the learning function of the testing animal model brain

and a maximum response was observed at the dose regimen of 80 mg/kg.

AUTHOR INFORMATION

Corresponding Author

Fareeha Anwar – Riphah Institute of Pharmaceutical Sciences, Riphah International University, Lahore 54000, Pakistan; orcid.org/0000-0001-5097-8128; Phone: +92-3338883251; Email: Fareeha.anwar@riphah.edu.pk

Authors

Wajeeha Waseem – Riphah Institute of Pharmaceutical Sciences, Riphah International University, Lahore 54000, Pakistan

Uzma Saleem – Faculty of Pharmaceutical Sciences, Government College University (GCU) Faisalabad, Faisalabad 38000, Pakistan; orcid.org/0000-0002-1541-4236

Bashir Ahmad – Riphah Institute of Pharmaceutical Sciences, Riphah International University, Lahore 54000, Pakistan

Rehman Zafar – Department of Pharmaceutical Chemistry, Faculty of Pharmaceutical Sciences, Riphah International University, Islamabad 44000, Pakistan

Asifa Anwar – Department of Pharmacy, Islamia University Bahawalpur, Bahawalpur 63100, Pakistan

Muhammad Saeed Jan – Department of Pharmacy, University of Swabi, Swabi 23430 KPK, Pakistan

Umer Rashid – Department of Chemistry, Comsat University, Abbottabad 22060, Pakistan; orcid.org/0000-0002-2419-3172

Abdul Sadiq – Department of Pharmacy, University of Malakand, Chakdara 18000 KPK, Pakistan

Tariq Ismail – Department of Pharmacy, COMSAT University, Abbottabad 22060, Pakistan

Complete contact information is available at:

<https://pubs.acs.org/10.1021/acsomega.2c03058>

Author Contributions

W.W. carried out the research work, analysis, and review and final drafting of the research paper. F.A. and B.A. supervised the project. R.Z. provided the compound after complete characterization. M.S.J., U.R., and A.S. helped in performing the pharmacological activities, ELISA, and computational studies.

Notes

The authors declare no competing financial interest. All data has been provided as original and no supporting files are available.

ACKNOWLEDGMENTS

All the authors acknowledge the contribution of the Department of Pharmacy, University of Malakand, Chakdara, Dir, KPK, for their support.

REFERENCES

- (1) Wan, Y.-W.; Al-Ouran, R.; Mangleburg, C. G.; Perumal, T. M.; Lee, T. V.; Allison, K.; Swarup, V.; Funk, C. C.; Gaiteri, C.; Allen, M. Meta-analysis of the Alzheimer's disease human brain transcriptome and functional dissection in mouse models. *Cell Rep.* **2020**, *32*, No. 107908.
- (2) Dubois, B.; Villain, N.; Frisoni, G. B.; Rabinovici, G. D.; Sabbagh, M.; Cappa, S.; Bejanin, A.; Bombois, S.; Epelbaum, S.; Teichmann, M.; Habert, M. O.; Nordberg, A.; Blennow, K.; Galasko, D.; Stern, Y.; Rowe, C. C.; Salloway, S.; Schneider, L. S.; Cummings, J. L.; Feldman,

H. H. Clinical diagnosis of Alzheimer's disease: recommendations of the International Working Group. *Lancet Neurol.* **2021**, *20*, 484–496.

- (3) Weller, J.; Budson, A., Current understanding of Alzheimer's disease diagnosis and treatment. *F1000Research* **2018**, *7*.

- (4) Tiwari, S.; Atluri, V.; Kaushik, A.; Yndart, A.; Nair, M. Alzheimer's disease: pathogenesis, diagnostics, and therapeutics. *Int. J. Nanomed.* **2019**, *14*, 5541.

- (5) Sun, Q.; Zhang, J.; Li, A.; Yao, M.; Liu, G.; Chen, S.; Luo, Y.; Wang, Z.; Gong, H.; Li, X. Acetylcholine deficiency disrupts extratelencephalic projection neurons in the prefrontal cortex in a mouse model of Alzheimer's disease. *Nat. Commun.* **2022**, *13*, 1–22.

- (6) Rad, S. K.; Arya, A.; Karimian, H.; Madhavan, P.; Rizwan, F.; Koshy, S.; Prabhu, G. Mechanism involved in insulin resistance via accumulation of β -amyloid and neurofibrillary tangles: Link between type 2 diabetes and Alzheimer's disease. *Drug Des., Dev. Ther.* **2018**, *12*, 3999.

- (7) Cao, J.; Hou, J.; Ping, J.; Cai, D. Advances in developing novel therapeutic strategies for Alzheimer's disease. *Mol. Neurodegener.* **2018**, *13*, 1–20.

- (8) Laurettil, E.; Praticò, D. Alzheimer's disease: Phenotypic approaches using disease models and the targeting of tau protein. *Expert Opin. Ther. Targets* **2020**, *24*, 319–330.

- (9) Sudha, R.; Sukumaran, K. Anti-Oxidants used for the Treatment of Alzheimer Disease. *Res. J. Pharm. Technol.* **2020**, *13*, 475–480.

- (10) Lu, M.-H.; Zhao, X.-Y.; Yao, P.-P.; Xu, D.-E.; Ma, Q.-H. The mitochondrion: a potential therapeutic target for Alzheimer's disease. *Neurosci. Bull.* **2018**, *34*, 1127–1130.

- (11) Bagherniya, M.; Nobili, V.; Blesso, C. N.; Sahebkar, A. Medicinal plants and bioactive natural compounds in the treatment of non-alcoholic fatty liver disease: a clinical review. *Pharmacol. Res.* **2018**, *130*, 213–240.

- (12) Schneider, L. S. Alzheimer disease pharmacologic treatment and treatment research. *CONTINUUM: Lifelong Learning in Neurology* **2013**, *19*, 339–357.

- (13) Gentner, T. X.; Mulvey, R. E. Alkali-Metal Mediation: Diversity of Applications in Main-Group Organometallic Chemistry. *Angew. Chem., Int. Ed.* **2021**, *60*, 9247–9262.

- (14) Witzke, R. J.; Chapovetsky, A.; Conley, M. P.; Kaphan, D. M.; Delferro, M. Nontraditional catalyst supports in surface organometallic chemistry. *ACS Catal.* **2020**, *10*, 11822–11840.

- (15) Robertson, S. D.; Uzelac, M.; Mulvey, R. E. Alkali-metal-mediated synergistic effects in polar main group organometallic chemistry. *Chem. Rev.* **2019**, *119*, 8332–8405.

- (16) Md Yusop, A. H.; Ulum, M. F.; Al Sakkaf, A.; Nur, H. Current Status and Outlook of Porous Zn-based Scaffolds for Bone Applications: A Review. *J. Bionic Eng.* **2022**, 1–751.

- (17) Piemontese, L.; Sergio, R.; Rinaldo, F.; Brunetti, L.; Perna, F. M.; Santos, M. A.; Capriati, V. Deep eutectic solvents as effective reaction media for the synthesis of 2-hydroxyphenylbenzimidazole-based scaffolds en route to donepezil-like compounds. *Molecules* **2020**, *25*, 574.

- (18) Delavaux-Nicot, B.; Ben Aziza, H.; Nierengarten, I.; Minh Nguyet Trinh, T.; Meichsner, E.; Chessé, M.; Holler, M.; Abidi, R.; Maisonhaute, E.; Nierengarten, J. F. A Rotaxane Scaffold for the Construction of Multiporphyrinic Light-Harvesting Devices. *Chem. - Eur. J.* **2018**, *24*, 133–140.

- (19) Dong, L.; Yang, W.; Tian, H.; Huang, Y.; Wang, X.; Xu, C.; Wang, C.; Kang, F.; Wang, G. Flexible and conductive scaffold-stabilized zinc metal anodes for ultralong-life zinc-ion batteries and zinc-ion hybrid capacitors. *Chem. Eng. J.* **2020**, *384*, No. 123355.

- (20) Vishvakarma, V. K.; Shukla, N.; Kumari, K.; Patel, R.; Singh, P. A model to study the inhibition of nsP2B-nsP3 protease of dengue virus with imidazole, oxazole, triazole thiazole, and thiazolidine based scaffolds. *Heliyon* **2019**, *5*, No. e02124.

- (21) Iyaswamy, A.; Wang, X.; Krishnamoorthi, S.; Kaliamoorthy, V.; Sreenivasamurthy, S. G.; Durairajan, S. S. K.; Song, J.-X.; Tong, B. C. K.; Zhu, Z.; Su, C. F. Theranostic F-SLOH mitigates Alzheimer's disease pathology involving TFEB and ameliorates cognitive functions in Alzheimer's disease models. *Redox biology* **2022**, *51*, No. 102280.

- (22) Iyaswamy, A.; Krishnamoorthi, S. K.; Zhang, H.; Sreenivasamurthy, S. G.; Zhu, Z.; Liu, J.; Su, C.-F.; Guan, X.-J.; Wang, Z.-Y.; Cheung, K.-H.; Song, J. X.; Durairajan, S. S. K.; Li, M. Qinyangshen mitigates amyloid- β and Tau aggregate defects involving PPAR α -TFEB activation in transgenic mice of Alzheimer's disease. *Phytomedicine* **2021**, *91*, No. 153648.
- (23) Kumari, S.; Dcunha, R.; Sanghvi, S. P.; Nayak, G.; Kalthur, S. G.; Raut, S. Y.; Mutalik, S.; Siddiqui, S.; Alrumman, S. A.; Adiga, S. K.; Kalthur, G. Organophosphorus pesticide quinalphos (Ekalux 25 EC) reduces sperm functional competence and decreases the fertilisation potential in Swiss albino mice. *Andrologia* **2021**, *53*, No. e14115.
- (24) Ayaz, M.; Sadiq, A.; Wadood, A.; Junaid, M.; Ullah, F.; Khan, N. Z. Cytotoxicity and molecular docking studies on phytosterols isolated from *Polygonum hydropiper* L. *Steroids* **2019**, *141*, 30–35.
- (25) Ahmad, A.; Ullah, F.; Sadiq, A.; Ayaz, M.; Jan, M. S.; Shahid, M.; Wadood, A.; Mahmood, F.; Rashid, U.; Ullah, R. Comparative cholinesterase, α -glucosidase inhibitory, antioxidant, molecular docking, and kinetic studies on potent succinimide derivatives. *Drug Des., Dev. Ther.* **2020**, *14*, 2165.
- (26) Tegin, İ.; Yabalak, E.; Sadik, B.; Fidan, M. Evaluation of chemical content and radical scavenging activity of *Allium Vineale* L. extract and its elemental analysis. *Rev. Roum. Chim.* **2019**, *64*, 673–679.
- (27) Re, R.; Pellegrini, N.; Proteggente, A.; Pannala, A.; Yang, M.; Rice-Evans, C. Antioxidant activity applying an improved ABTS radical cation decolorization assay. *Free Radical Biol. Med.* **1999**, *26*, 1231–1237.
- (28) Zafar, R.; Zubair, M.; Ali, S.; Shahid, K.; Waseem, W.; Naureen, H.; Haider, A.; Jan, M. S.; Ullah, F.; Sirajuddin, M.; Sadiq, A. Zinc metal carboxylates as potential anti-Alzheimer's candidate: in vitro anticholinesterase, antioxidant and molecular docking studies. *J. Biomol. Struct. Dyn.* **2021**, *39*, 1044–1054.
- (29) Jan, M. S.; Ahmad, S.; Hussain, F.; Ahmad, A.; Mahmood, F.; Rashid, U.; Ullah, F.; Ayaz, M.; Sadiq, A. Design, synthesis, in-vitro, in-vivo and in-silico studies of pyrrolidine-2, 5-dione derivatives as multitarget anti-inflammatory agents. *Eur. J. Med. Chem.* **2020**, *186*, No. 111863.
- (30) Jacobs, B. Y.; Allen, K. D. Factors affecting the reliability of behavioral assessments for rodent osteoarthritis models. *Lab. Anim.* **2020**, *54*, 317–329.
- (31) Iyaswamy, A.; Krishnamoorthi, S.; Liu, Y.; Song, J.; Kammala, A.; Sreenivasamurthy, S.; Malampati, S.; Tong, B.; Selvarasu, K.; Cheung, K.; Lu, J. H.; Tan, J. Q.; Huang, C. Y.; Durairajan, S. S. K.; Li, M. Yuan-Hu Zhi Tong Prescription Mitigates Tau Pathology and Alleviates Memory Deficiency in the Preclinical Models of Alzheimer's Disease. *Frontiers in Pharmacology* **2020**, *11*, No. 584770.
- (32) Knight, P.; Chellian, R.; Wilson, R.; Behnood-Rod, A.; Panunzio, S.; Bruijnzeel, A. W. Sex differences in the elevated plus-maze test and large open field test in adult Wistar rats. *Pharmacol., Biochem. Behav.* **2021**, *204*, No. 173168.
- (33) Zhao, Y.; Lu, F.; Zhang, Y.; Zhang, M.; Zhao, Y.; Luo, J.; Kong, H.; Qu, H. Water-Soluble Carbon Dots in Cigarette Mainstream Smoke: Their Properties and the Behavioural, Neuroendocrinological, and Neurotransmitter Changes They Induce in Mice. *Int. J. Nanomed.* **2021**, *16*, 2203.
- (34) Sreenivasamurthy, S. G.; Iyaswamy, A.; Krishnamoorthi, S.; Senapati, S.; Malampati, S.; Zhu, Z.; Su, C.-F.; Liu, J.; Guan, X.-J.; Tong, B. C.-K.; Cheung, K. H.; Tan, J. Q.; Lu, J. H.; Durairajan, S. S. K.; Song, J. X.; Li, M. Protopine promotes the proteasomal degradation of pathological tau in Alzheimer's disease models via HDAC6 inhibition. *Phytomedicine* **2022**, *96*, No. 153887.
- (35) Bromley-Brits, K.; Deng, Y.; Song, W. Morris water maze test for learning and memory deficits in Alzheimer's disease model mice. *JoVE (Journal of Visualized Experiments)* **2011**, *53*, No. e2920.
- (36) Tucker, L. B.; Velosky, A. G.; McCabe, J. T. Applications of the Morris water maze in translational traumatic brain injury research. *Neurosci. Biobehav. Rev.* **2018**, *88*, 187–200.
- (37) Das, P.; Manna, I.; Biswas, A. K.; Bandyopadhyay, M. Exogenous silicon alters ascorbate-glutathione cycle in two salt-stressed indica rice cultivars (MTU 1010 and Nonabokra). *Environ. Sci. Pollut. Res.* **2018**, *25*, 26625–26642.
- (38) Milek, J. Estimation of the kinetic parameters for H₂O₂ enzymatic decomposition and for catalase deactivation. *Braz. J. Chem. Eng.* **2018**, *35*, 995–1004.
- (39) Nazir, S.; Anwar, F.; Saleem, U.; Ahmad, B.; Raza, Z.; Sanawar, M.; Ismail, T. Drotaverine Inhibitor of PDE4: Reverses the Streptozotocin Induced Alzheimer's Disease in Mice. *Neurochem. Res.* **2021**, *46*, 1814–1829.
- (40) Sahu, R.; Meghavarnam, A. K.; Janakiraman, S. Response surface methodology: An effective optimization strategy for enhanced production of nitrile hydratase (NHase) by *Rhodococcus rhodochrous* (RS-6). *Heliyon* **2020**, *6*, No. e05111.
- (41) Tayyab Imtiaz, M.; Anwar, F.; Saleem, U.; Ahmad, B.; Hira, S.; Mehmood, Y.; Bashir, M.; Najam, S.; Ismail, T. Triazine Derivative as Putative Candidate for the Reduction of Hormone-Positive Breast Tumor: In Silico, Pharmacological, and Toxicological Approach. *Front. Pharmacol.* **2021**, *12*, 1267.
- (42) Mazumder, M. K.; Paul, R.; Bhattacharya, P.; Borah, A. Neurological sequel of chronic kidney disease: From diminished Acetylcholinesterase activity to mitochondrial dysfunctions, oxidative stress and inflammation in mice brain. *Sci. Rep.* **2019**, *9*, 1–22.
- (43) Singh, V.; Chauhan, G.; Shri, R. Anti-depressant like effects of quercetin 4'-O-glucoside from *Allium cepa* via regulation of brain oxidative stress and monoamine levels in mice subjected to unpredictable chronic mild stress. *Nutr. Neurosci.* **2021**, *24*, 35–44.
- (44) Zafar, R.; Shahid, K.; Wilson, L. D.; Fahid, M.; Sartaj, M.; Waseem, W.; Saeed Jan, M.; Zubair, M.; Irfan, A.; Ullah, S.; Sadiq, A. Organotin (IV) complexes with sulphonyl hydrazide moiety. Design, synthesis, characterization, docking studies, cytotoxic and anti-leishmanial activity. *J. Biomol. Struct. Dyn.* **2021**, 1–11.
- (45) Vasquez-Bonilla, W. O.; Orozco, R.; Argueta, V.; Sierra, M.; Zambrano, L. I.; Muñoz-Lara, F.; López-Molina, D. S.; Arteaga-Livias, K.; Grimes, Z.; Bryce, C.; Paniz-Mondolfi, A.; Rodríguez-Morales, A. J. A review of the main histopathological findings in coronavirus disease 2019. *Human pathology* **2020**, *105*, 74–83.
- (46) Akinyemi, A. J.; Oboh, G.; Ogunsuyi, O.; Abolaji, A. O.; Udofia, A. Curcumin-supplemented diets improve antioxidant enzymes and alter acetylcholinesterase genes expression level in *Drosophila melanogaster* model. *Metabolic brain disease* **2018**, *33*, 369–375.